Thoracic Magnetic Resonance Imaging Applications in Children

Adem Karaman

ABSTRACT

Lung pathologies in the pediatric population can usually be detected using chest radiography. Multidetector computed tomography (MDCT) imaging is often used as a supplementary method in the evaluation of lung diseases. Recently, magnetic resonance imaging (MRI) techniques were found to be reliable in the evaluation of pulmonary diseases in the pediatric population. This review study describes the routine application of MRI examinations and the use of thoracic MRI with a particular focus in pediatric patients.

Keywords: Children, magnetic resonance imaging, lung

Introduction

Lung pathologies in the pediatric population can usually be detected with the use of chest radiography. Multidetector computed tomography (MDCT) imaging is often used as a supplementary method in the evaluation of lung diseases. Furthermore, MDCT imaging is the preferred initial imaging modality for a detailed evaluation of lung diseases in children [1-3].

Traditionally, assessment of the thorax using magnetic resonance imaging (MRI) was limited due to low proton density, which yields weak signals [4-6]. Recently, nevertheless, MRI has been recognized as having utility in the evaluation of lung diseases in the pediatric population. Owing to the inherent soft tissue contrast, thoracic MRI can be performed without contrast media administration [7-9]. This development has also been supported by the option of MRI, under free-breathing conditions, which is very important in the pediatric population [7, 10].

Therefore, the morphological and functional evaluation of lung diseases in children by MRI may provide an alternative to MDCT imaging. This study aims to provide a brief overview of the uses and effectiveness of thoracic MRI in the pediatric population.

General Principles, Artifacts, and Sequence Protocols

Thoracic MRI has long been challenging due to the magnetically heterogeneous environment of the thorax. The lung parenchyma is a low proton-density structure and has a low signal-to-noise ratio. Furthermore, cardiac and respiratory motion artifacts can lead to difficulty in obtaining any reproducible thoracic MRI data, which is a critical issue [11-15]. Thus, T2-weighted sequences are essential in thoracic MRI. Recent studies usually refer to triggered T2-weighted turbo spin echo (TSE) sequences with a long echo train and T2-weighted half-Fourier acquisition single-shot turbo spin-echo sequences, which are usually emphasized (Figure 1). Axial T1-weighted 3D-GRE (VIBE) sequence with high sensitivity for small lesions is acquired in a single-breath hold, whereas axial T2-weighted short tau inversion recovery with a multibreath hold method is used to detect enlarged lymph nodes and skeletal lesions [7,16].

Indications for Thoracic MRI in Children

Lung Diseases with Alveolar Involvement

Pneumonia is a typical example of lung parenchymal disease with alveolar involvement. Its pathologies can be dependably detected using T2-weighted sequences. Using MRI, all processes that appear as opacification on X-ray images, such as alveolar infiltration and exudation patterns, can usually be

Cite this article as: *Karaman A. Thoracic Magnetic Resonance Imaging Applications in Children. Eurasian J Med 2020; 52(1): 94-7.*

Department of Radiology, Ataturk University School of Medicine, Erzurum, Turkey

Received: November 13, 2019
Accepted: December 15, 2019

Correspondence to: Adem Karaman
E-mail: drkaraman77@yahoo.com

DOI 10.5152/eurasianjmed.2020.19236

evaluated more definitively and without summation effects. Therefore, thoracic MRI exhibits a remarkable diagnostic advantage over radiographs. MRI is also suitable for detecting complications of lung parenchymal infiltrations [14-18].

Lung Diseases with Interstitial Involvement

Interstitial parenchymal pathologies can often be detected using MDCT; however, MRI results of these pathologies sometimes differ remarkably from those of high-resolution MDCT. Acute interstitial lung diseases that involve infections and edema with interstitial infiltration can be recognized as a signal increase on T2-weighted MRI (Figure 2). When these cellular and capillary structures decrease, the MRI of pulmonary fibrosis will reveal low signal intensity on T2-weighted images [19, 20].

Lung Neoplasia

Primary thoracic neoplasias are rare in the pediatric population, so there have been no clinical studies on the use of MRI in this context. In addition, most of the lung tumors are metastatic (Figures 3, 4). Benign lesions, such as thymoma or hemangioma, are sometimes detected (Figures 5, 6). MDCT is generally preferred as the gold standard in parenchymal metastasis detection. Thus, thoracic MRI has so far been used in the pediatric population solely to monitor the regression of known lung metastatic tumors. MRI can detect parenchymal nodules larger than 5 mm [3, 9, 14].

Lung Malformations

Pulmonary sequestrations are rare congenital lung malformations. Pulmonary sequestration with aberrant feeding vessel can be accurately diagnosed by magnetic resonance angiography (MRA). The main differential diagnosis is cystic adenomatoid malformation, which does not have an atypical vessel. MDCT has no diagnos-

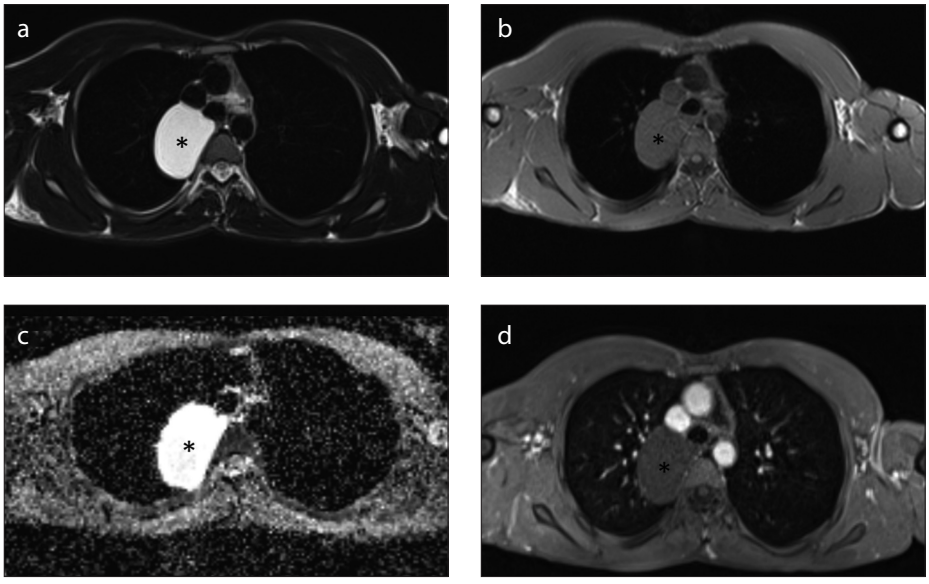

Figure 1. a-d. A 13-year-old female with a bronchogenic cyst in the right upper lobe. Axial T2-weighted fat-suppressed image (a) reveals a hyperintense bronchogenic cyst (black asterisk). Axial T1-weighted image (b) reveals a hypointense bronchogenic cyst (black asterisk). Axial diffusion-weighted (ADC map) image (c) exhibits no diffusion restriction (black asterisk). Axial postcontrast enhanced T1-weighted image (d) exhibits no contrast enhancement (black asterisk).

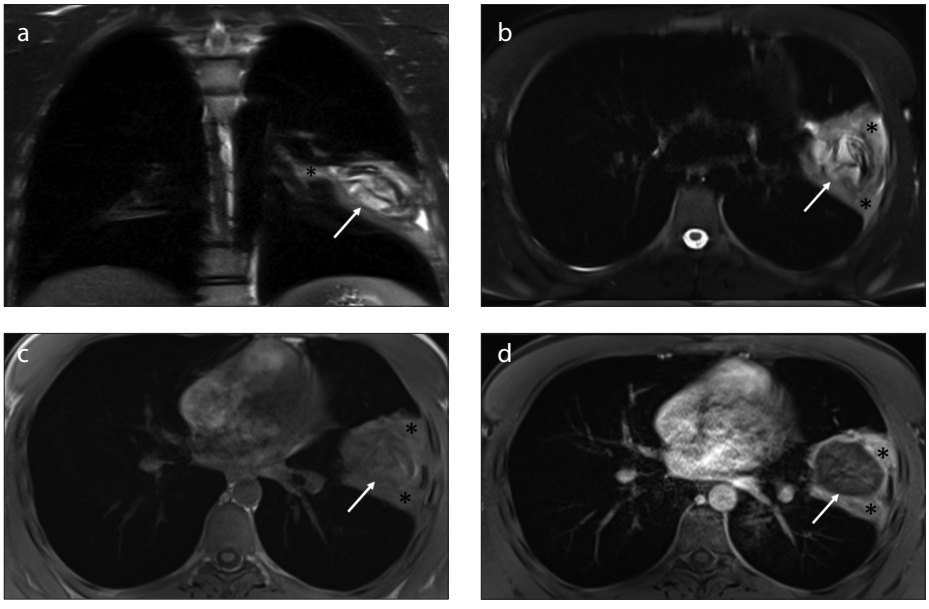

Figure 2. a-d. A 15-year-old male with a ruptured hydatid cyst in the left lower lobe anteromedial segment. Coronal T2-weighted (a), axial T2-weighted fat-suppressed (b), and axial T1-weighted (c) images reveal the hydatid cyst (white arrow) and intense inflammation secondary to rupture (black asterisk). Axial postcontrast-enhanced image (d) reveals no contrast enhancement in the hydatid cyst lesion (white arrow) and distinct contrast enhancement in the inflammation secondary to rupture (black asterisk).

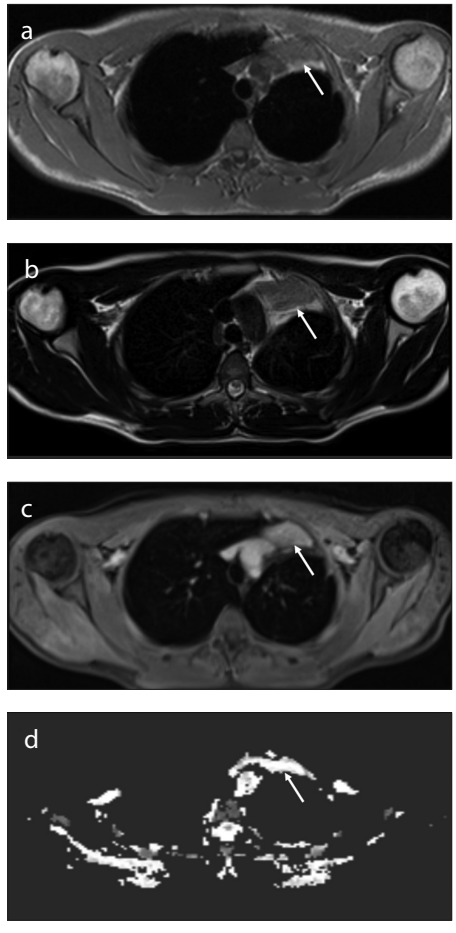

Figure 3. a-d. A 12-year-old male with a pathologically confirmed carcinoid tumor in the left upper lobe. Axial T1-weighted image (a) reveals the iso-hypointense carcinoid tumor (white arrow). Axial T2-weighted image (b) reveals a hypointense carcinoid tumor (white arrow). Axial postcontrast enhancement T1-weighted image (c) reveals contrast enhancement in carcinoid tumor (white arrow). Axial diffusion-weighted (ADC map) image (d) reveals no diffusion restriction (white arrow).

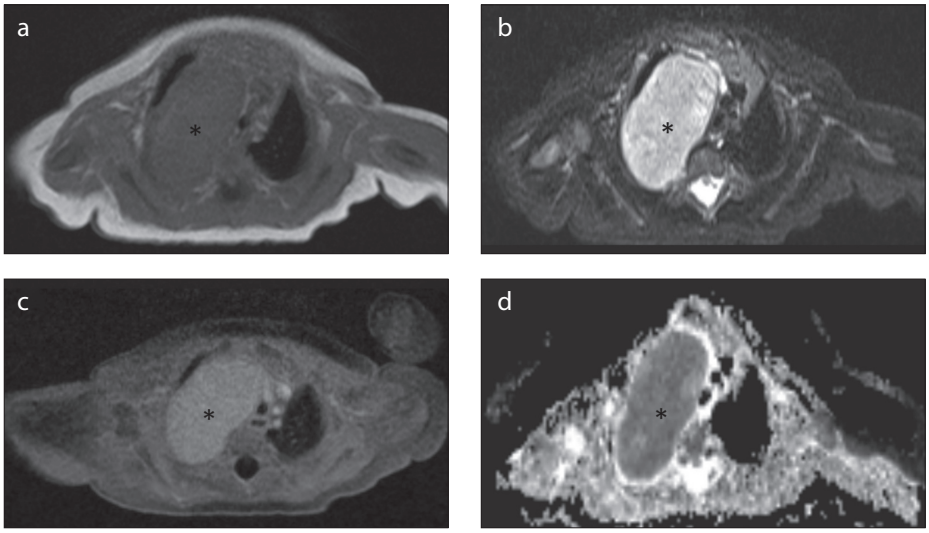

Figure 4. a-d. A 9-year-old female with pathologically confirmed neuroblastoma in the right upper lobe. Axial T1-weighted image (a) reveals hypointense neuroblastoma lesion (black asterisk). Axial T2-weighted image (b) reveals a hyperintense neuroblastoma lesion (black asterisk). Axial postcontrast-enhanced T1-weighted image reveals a distinct contrast enhancement in neuroblastoma lesion (black asterisk). Axial diffusion-weighted (ADC map) image (d) reveals diffusion restriction in the neuroblastoma lesion (black asterisk).

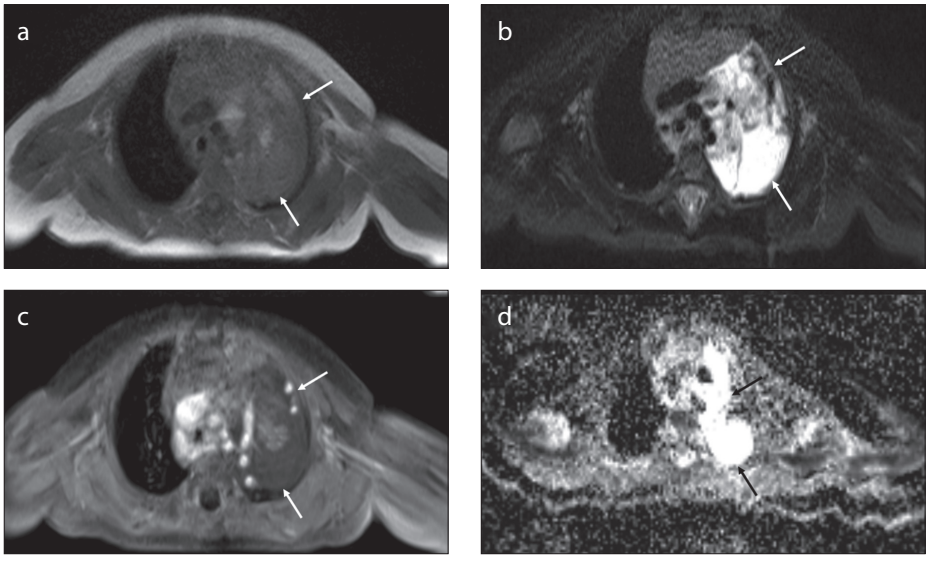

Figure 5. a-d. An 8-year-old male with pathologically confirmed cavernous hemangioma in the left upper lobe. Axial T1-weighted (a) and T2-weighted (b) images reveal the cavernous hemangioma lesion (white arrows). Axial postcontrast-enhanced T1-weighted image (c) reveals peripheral and internal contrast enhancement in the cavernous hemangioma lesion (white arrows). Axial diffusion-weighted (ADC map) image (d) reveals no diffusion restriction (white arrows).

tic advantage over MRI in this context. Thoracic MRI is recommended for the diagnosis of type III cystic adenomatoid malformations that involve small and solid cysts [3, 14].

Cystic Fibrosis

MRI can be performed to detect the typical findings of cystic fibrosis in children, such as bronchial wall thickening, bronchiectasis, mucus plugging, and consolidations. T2-weighted sequences with respiratory gating are recommended to identify mucus-filled airways and enflamed bronchial walls [20-22].

Pulmonary Hypoplasia and Aplasia

Pulmonary hypoplasia or aplasia is a congenital disorder that involves incomplete development of the lung parenchyma. In pulmonary hypoplasia, the pulmonary artery is congenitally small and can be detected by MRA. Respiratory and cardiac-gated bright-blood imaging methods are also suitable for identifying small bronchial structures [3, 23, 24].

Pectus Excavatum

Assessment of pectus excavatum, a congenital concavity of the sternum and cartilages, ideally

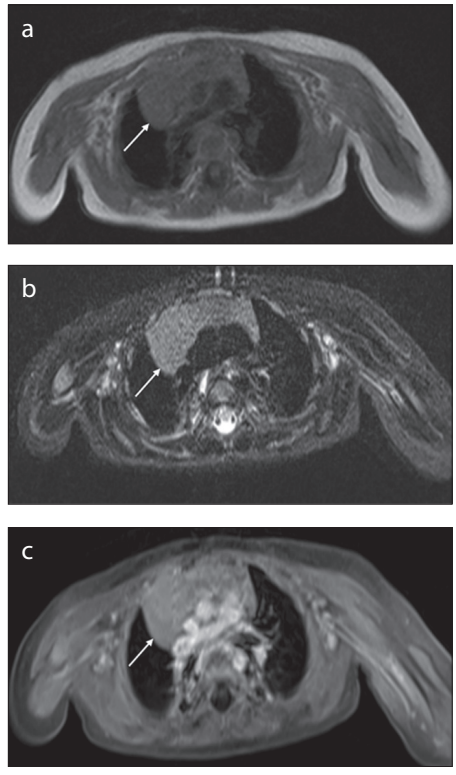

Figure 6. a-c. An 11-year-old male with pathologically confirmed thymoma in the anterior mediastinum. Axial T1-weighted image (a) reveals hypointense thymoma lesion (white arrow). Axial T2-weighted image (b) reveals hyperintense thymoma lesion (white arrow). Axial postcontrast-enhanced T1-weighted image (c) reveals no contrast enhancement in the thymoma lesion (white arrow).

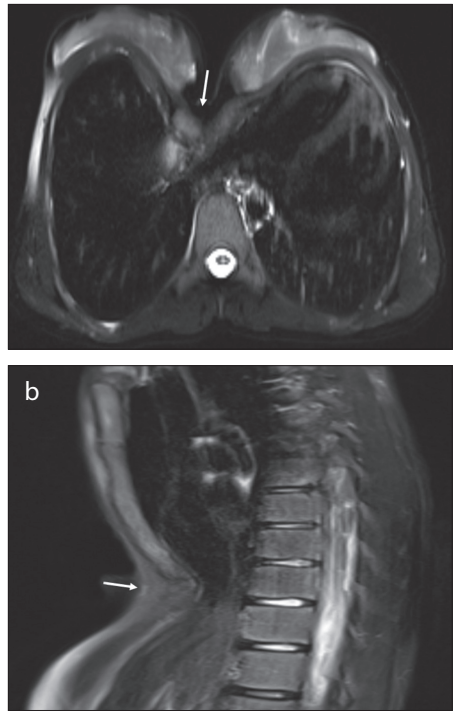

Figure 7. a, b. A 14-year-old female with pectus excavatum. Axial T2-weighted (a) and sagittal T2-weighted (b) images reveal the pectus excavatum deformity (white arrows).

includes a careful anatomical description using imaging modalities to detect the depth of depression and extent of cardiac compression (Figure 7). The pectus severity index, described in 1973, is obtained by dividing the internal transverse distance of the thorax by the vertebral–sternal distance at the point of most significant depression, measured by computed tomography imaging. Nevertheless, thoracic MRI is also a good option for evaluating this deformity [25, 26].

Conclusion

In children, MRI of the thorax provides more useful data for diagnosis than radiography. In many cases, thoracic MRI can replace radiography and MDCT, thereby reducing the children's exposure to ionizing radiation. T2-weighted TSE sequences and respiratory gating procedures, in particular, make MRI an essential imaging modality with broad applicability in pediatric thoracic imaging. Therefore, MRI should be considered as an alternative to MDCT in the evaluation of lung diseases in children.

Ethics Committee Approval: Ethics committee approval was received for this study from the ethics committee of the Ethics Committee of Erzurum Regional Training and Research Hospital.

Peer-review: Externally peer-reviewed.

Conflict of Interest: The author has no conflicts of interest to declare.

Financial Disclosure: The author declared that this study has received no financial support.

References

1. Brenner D, Elliston C, Hall E, et al. Estimated risks of radiation-induced fatal cancer from pediatric CT. Am J Roentgenol 2001; 176: 289-96. [CrossRef]
2. Pirimoglu B, Sade R, Ogul H, Kantarci M, Eren S, Levent A. How Can New Imaging Modalities Help in the Practice of Radiology? Eurasian J Med 2016; 48: 213-21. [CrossRef]
3. Alper F, Kurt AT, Aydin Y, Ozgokce M, Akgun M. The role of dynamic magnetic resonance imaging in the evaluation of pulmonary nodules and masses. Med Princ Pract 2013; 22: 80-6. [CrossRef]
4. Fain SB, Korosec FR, Holmes JH, et al. Functional lung imaging using hyperpolarized gas MRI. J Magn Reson Imaging 2007: 25: 910-23. [CrossRef]
5. Yildiz GA, Yapca OE, Al RA, Ingec M. Congenital Ewing's Sarcoma, a Rare and Difficult Diagnosis: A Case Report. Eurasian J Med 2018; 50: 202-3. [CrossRef]
6. Lee EY. Advancing CT and MR imaging of the lungs and airways in children: imaging into practice. Pediatr Radiol 2008; 38: 208-12. [CrossRef]
7. PuderbachM, Hintze C, Ley S, et al. MR imaging of the chest: a practical approach at 1.5 T. Eur J Radiol 2007; 64: 345-55. [CrossRef]
8. Karaman A, Araz O, Durur-Subasi I, et al. Added value of DCE-MRI in the management of cystic-cavitary lung lesions. Respirology 2016; 21: 739-45. [CrossRef]
9. Karaman A, Durur-Subasi I, Alper F, Durur-Karakaya A, Subasi M, Akgun M. Is it better to include necrosis in apparent diffusion coefficient (ADC) measurements? The necrosis/wall ADC ratio to differentiate malignant and benign necrotic lung lesions: Preliminary results. J Magn Reson Imaging 2017; 46: 1001-6. [CrossRef]
10. Karaman A, Kahraman M, Bozdoğan E, Alper F, Akgün M. [Diffusion magnetic resonance imaging of thorax]. Tuberk Toraks 2014; 62: 215-30.
11. Swift AJ, Woodhouse N, Fichele S, et al. Rapid lung volumetry using ultrafast dynamic magnetic resonance imaging during forced vital capacity maneuver: correlation with spirometry. Invest Radiol 2007; 42: 37-41. [CrossRef]
12. Hirsch W, Sorge I, Schluter A, et al. Assessment of pulmonary air trapping and obstruction in expiration: an experimental MRI study. Magn Reson Imaging 2005; 23: 991-4. [CrossRef]
13. Hatabu H, Chen Q, Stock KW, et al. Fast magnetic resonance imaging of the lung. Eur J Radiol 1999; 29: 114-32. [CrossRef]
14. Hirsch W, Sorge I, Krohmer S, Weber D, Meier K, Till H. MRI of the lungs in children. Eur J Radiol 2008; 68: 278-88. [CrossRef]
15. Peker E, Sonmez DY, Akkaya HE, Hayme S, Erden MI, Erden A. Diagnostic Performance of Multiparametric MR Imaging at 3.0 Tesla in Discriminating Prostate Cancer from Prostatitis: A Histopathologic Correlation. Eurasian J Med 2019; 51: 31-37. [CrossRef]
16. Bruegel M, Gaa J, Woertler K, et al. MRI of the lung: value of different turbo spin-echo, single-shot turbo spin-echo, and 3D gradient-echo pulse sequences for the detection of pulmonary metastases. J Magn Reson Imaging 2007; 25: 73-81. [CrossRef]
17. Amundsen T, Torheim G,Waage A, et al. Perfusion magnetic resonance imaging of the lung: characterisation of pneumonia and chronic obstructive pulmonary disease. J Magn Reson Imaging 2000; 11: 622-8.
18. Lutterbey G, Wattjes MP, Doerr D, et al. Atelectasis in children undergoing either propofol infusion or positive pressure ventilation anesthesia for magnetic resonance imaging. Paediatr Anaesth 2007; 17: 121-5. [CrossRef]
19. Karaman A, Durur-Subasi I, Alper F, et al. Correlation of diffusion MRI with the Ki-67 index in non-small cell lung cancer. Radiol Oncol 2015; 49: 250-5. [CrossRef]
20. Altes TA, Eichinger M, Puderbach M. Magnetic resonance imaging of the lung in cystic fibrosis. Proc Am Thorac Soc 2007; 4: 321-7. [CrossRef]
21. Puderbach M, Eichinger M, Haeselbarth J, et al. Assessment of morphological MRI for pulmonary changes in cystic fibrosis (CF) patients: comparison to thin-section CT and chest x-ray. Invest Radiol 2007; 42: 715-25. [CrossRef]
22. Anjorin A, Schmidt H, Posselt HG, et al. Comparative evaluation of chest radiography, low-field MRI, the Shwachman-Kulczycki score and pulmonary function tests in patients with cystic fibrosis. Eur Radiol 2008; 18: 1153-61. [CrossRef]
23. Fenchel M, Greil GF, Martirosian P, et al. Three-dimensional morphological magnetic resonance imaging in infants and children with congenital heart disease. Pediatr Radiol 2006; 36: 1265-72. [CrossRef]
24. Berrocal T, Madrid C, Novo S, et al. Congenital anomalies of the tracheobronchial tree, lung, and mediastinum: embryology, radiology, and pathology. Radiographics 2004; 24: e17. [CrossRef]
25. Nakagawa Y, Uemura S, Nakaoka T, et al. Evaluation of the Nuss procedure using pre- and postoperative computed tomographic index. J Pediatr Surg 2008; 43: 518-21. [CrossRef]
26. Herrmann KA, Zech C, Strauss T, et al. Cine MRI of the thorax in patients with pectus excavatum. Radiologe 2006; 46: 309-16. [CrossRef]